JCTC Journal of Chemical Theory and Computation

ARTICLE

pubs.acs.org/JCTC

Evaluation of the Nonlinear Optical Properties for Annulenes with Hückel and Möbius Topologies

Miquel Torrent-Sucarrat,*[,†] Josep M. Anglada,[†] and Josep M. Luis[‡]

[†]Departament de Química Biològica i Modelització Molecular, Institut de Química Avançada de Catalunya (IQAC−CSIC), c/Jordi Girona 18, E-08034 Barcelona, Spain

[‡]Institut de Química Computacional and Departament de Química, Universitat de Girona, E-17071 Girona, Catalonia, Spain

Supporting Information

ABSTRACT: Recently, much attention has been focused on the design and synthesis of molecules with aromatic Möbius topology. One of the most promising applications is the manufacture of Hückel-to-Möbius topological optical switches with high nonlinear optical properties. In this work, we evaluate the electronic and vibrational contributions to static and dynamic nonlinear optical properties of the C_S Hückel and C_2 Möbius topologies synthesized by Herges and co-workers (Ajami, D. et al. *Nature* **2003**, *426*, 819). Calculations are performed at the HF, B3LYP, BHandHLYP, BMK, M052X, CAM-B3LYP, and MP2 levels with the 6-31+G(d) basis set. Our results conclude that the BHandHLYP, M052X, and CAM-B3LYP methods correctly reproduce the X-ray crystal structure and provide similar nonlinear optical properties.

1. INTRODUCTION

The stability of a molecular conformation is the result of different interactions, e.g., steric effect, presence of a number of hydrogen bonds, stacking interactions, and conjugation. When discussing the overall effect of these interactions, *aromaticity*[1] has often been a guiding principle. This concept has been one of the most controversial and debated issues in chemistry during the past two decades.[2] According to the well-know Hückel rule, an aromatic (hydrocarbon) compound is a cyclic planar molecular structure stabilized by the delocalization of $4n + 2$ π electrons. On the other hand, if the planar molecule contains $4n$ π electrons, it is antiaromatic. However, the $4n + 2$ Hückel rule is not always fulfilled by the nonplanar molecules. In 1964, the seminal work of Heilbronner[3] showed that the Hückel rule is reversed for π chemical systems with an odd number of half-twists. Heilbronner, based on Hückel molecular orbital theory, predicts that singlet annulenes with $4n$ π electrons would be aromatic systems in twisted conformations where the p orbitals lie on the surface of a Möbius strip, whereas singlet $[4n + 2]$ Möbius molecules would be antiaromatic.

The concept of Möbius aromaticity has become very popular in the literature.[4] However, the synthesis of a viable[5] aromatic Möbius system has been a challenge for 40 years. The difficulty of this synthesis resides in the curvature of the system, resulting in a destabilization due to the *ring strain* being larger than the stabilization due to the *Möbius aromaticity*. In order to reduce this ring strain, large cyclic molecules can be envisaged, although the structures become more flexible and can flip back to the less-strained and stable Hückel topology.

The first experimental evidence for an aromatic Möbius system was obtained in 1971 with a short-lived intermediate, the charged cyclic 8 π electron [9]annulene, $(C_9H_9)^+$.[6] In 1998, Scheleyer et al.[7] reported theoretical support of the aromaticity of this species using geometric and magnetic criteria. A recent study[8] has shown that high-level coupled cluster calculations predict that Hückel and Möbius isomers of $(C_9H_9)^+$ are quasidegenerate (the energy difference is only 0.04 kcal mol^{-1}). Although experimental results[8] indicate that the Hückel structure is the most stable conformation since it is the unique conformer detected, it was considered that the Möbius structure could exist in small concentrations below the detection limit.

In 2003, Herges and co-workers[9] synthesized the first stable crystalline Möbius molecule combining a normal planar conjugated structure (with p orbitals orthogonal to the ring plane) and a rigid prefabricated belt-shaped conjugated segment (with p orbitals within the ring plane).[9−11] The suprafacial−suprafacial allowed [2 + 2] addition of syn-tricyclooctadiene and tetradehydrodianthracene followed by a thermal suprafacial−antarafacial cycloreversion leads to the isolation of five-ring opened isomers of bianthraquinodimethane modified [16] annulene. Two of them have Möbius topology (C_1 and C_2 symmetry, structure **2**), and one of them shows a Hückel topology (C_S symmetry, structure **1**, see Figure 1). The last two of them were isolated, but their structures could not be unequivocally elucidated. The aromaticity of these Möbius conformations has been a controversial issue, and it has been analyzed in different research groups,[9,11,12] which concluded that they show a weak aromaticity.

The difficulty in synthesizeing Möbius conformers with annulene systems arises from the small cis−trans isomerization barriers,[13] and then alternative systems have been studied. For instance, the possibility of charged annulene anions and cations has been screened.[14] Finally, the class of molecules that has succeeded in the creation of Möbius aromatic systems has been the expanded porphyrins,[15] macrocycles of pyrrolic subunits, and their analogues (benziporphyrins, vacataporphyrins). The conformational flexibility, the number and the nature of substituents

Received: August 2, 2011
Published: October 14, 2011

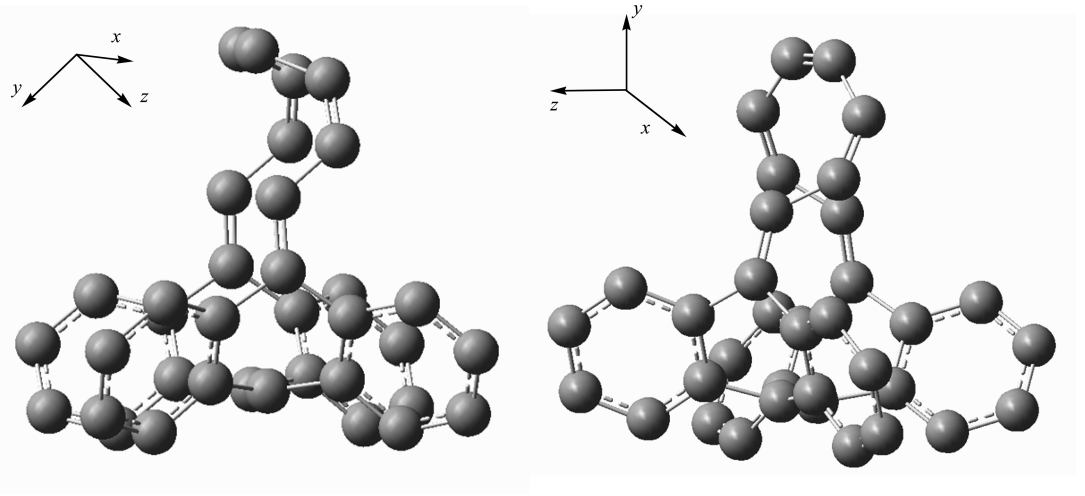

Hückel (C_S) **1** **Möbius** (C_2) **2**

Figure 1. CAM-B3LYP/6-31+G(d) optimized geometries of C_S Hückel and C_2 Möbius topologies of bianthraquinodimethane modified [16] annulene. The hydrogen atoms have been omitted for clarity.

on the pyrrolic and meso positions, and the metalation of the porphyrins allow them to achieve different topologies with distinct aromaticities and electronic properties.[16−18]

One of the most appealing applications is the possibility of switching between Möbius and Hückel topologies, applying only small changes in the external conditions or in the structure of the ring. The Möbius and Hückel molecules may have different electronic structures and properties. Specifically, the expanded porphyrins present a clear relationship between aromaticity, molecular geometry, and nonlinear optical properties (NLOP).[19] Then, topologically switchable porphyrins open the possibility of designing new optical switches. The key factors, which will determine their potential use as optical switches, will be the high values and the large differences of the NLOP between the Möbius and Hückel conformations.

The experimental results reported in the literature about NLOPs of Möbius−Hückel conformers show that they are very promising in the potential use as optical switches, although they only contain two-photon absorptions cross-section values. Computational chemistry is a useful tool for the evaluation of different static and dynamic NLO properties, e.g., the optical Kerr effect (OKE), electric-field-induced second harmonic generation (ESHG), and the intensity-dependent refractive index (IDRI). Xu et al.[20] studied the electronic dipole moment, polarizability, and first hyperpolarizability of four knot isomers of a cyclacene composed of 15 nitrogen-substituted benzo rings using the BHandHLYP/6-31+G(d) level. The four knot isomers are a Hückel cyclacene without a knot, a Möbius cyclacene with one knot, a Hückel cyclacene with two knots, and a Möbius cyclacene with three knots. The reported results show that the static electronic first polarizability values of cyclacenes with an odd number of knots (Möbius) can be 1 order of magnitude larger than those with an even number of knots (Hückel).

Using a clamped nucleus approximation,[21] the polarizability and hyperpolarizabilities can be decomposed into electronic and vibrational contributions.[22] Although neglected in the past, the vibrational contribution to the hyperpolarizabilities can be similar and even larger than the electronic counterpart.[23−27]

The choice of a theoretical approach for the evaluation of NLOP is not an easy task. For instance, the desirable coupled cluster methods are computationally prohibitive for these Möbius−Hückel topologocial switches, and the MP2 could only used for benchmarking purposes. Then, the only possible alternative method is density functional theory (DFT). However, it is well-know that an incorrect electric field dependence modeled by the exchange functional (in the conventional DFT methods) provokes an overestimation of the hyperpolarizabilities of chain-like molecules.[28] This deficiency can be alleviated using DFT functionals with a large fraction of Hartree−Fock (i.e., BMK, BHandHLYP, M052X)[29] or using new DFT functionals. Among them, it is important to remark on the long-range corrected functionals, which introduce a growing fraction of exact exchange when the distance increases, e.g., long-range corrected functional and the Coulomb-attenuating method (CAM).[30] These methods have become a promising tool for the evaluation of NLOP[27,31−33] and chiroptical properties.[34]

This work has two main goals: first, to report as far as we know the first exhaustive evaluation of the electronic and vibrational contributions to static and dynamic NLOP for a system with Hückel and Möbius topologies and, second, to search for a DFT level of theory capable of providing semiquantitative accuracy of the NLOP with a π-conjugated Hückel−Möbius switch. We have chosen the C_S Hückel (structure **1**, see Figure 2) and C_2 Möbius (structure **2**) topologies of bianthraquinodimethane modified [16] annulene synthesized by Herges and coworkers.[9,11] The moderate number of atoms of these systems allows a systematic study using different theoretical approaches.

2. COMPUTATIONAL METHODS

The evaluation of the electronic contribution to the dipole moment (μ^e), linear polarizability (α^e), first hyperpolarizability (β^e), and second hyperpolarizability (γ^e) were performed at the HF, B3LYP,[35] BHandHLYP,[36] BMK,[37] M052X,[38] CAM-B3LYP,[39] and MP2[40] levels with the 6-31+G(d)[41] basis set using the Gaussian 09 program package.[42] All of the NLOPs have been

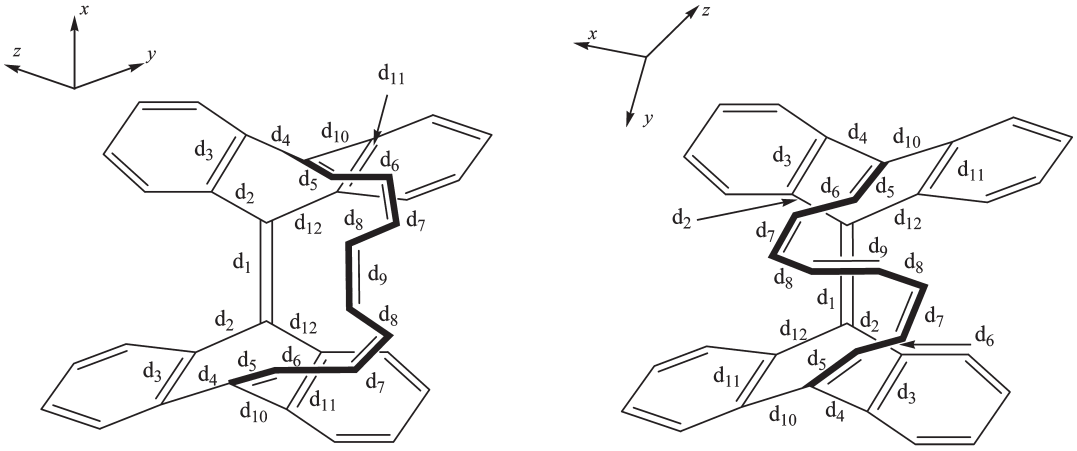

Hückel (C_S) **1** **Möbius** (C_2) **2**

Figure 2. Representation of C_S Hückel and C_2 Möbius topologies of bianthraquinodimethane modified [16] annulene. The labels are the bond distances displayed in the Tables 1 and 2.

evaluated in the gas phase.[43] μ^e, α^e, and β^e were analytically evaluated for all of the methodologies, except for the MP2 level, the level at which only μ^e was obtained analytically due to computational limitations. All remaining high-order properties (i.e., γ^e for HF and DFT methods and α^e, β^e, and γ^e for the MP2 level) were obtained by finite field differentiation of the highest-order analytical electronic contribution available. The numerical differentiation was carried out for field strengths of ±0.0002, ±0.0004, ±0.0008, and ±0.0016 au. The smallest field magnitude that produced a stable derivative was selected using a Romberg method triangle.[44] The symmetry restrictions have not been considered in the optimization process, and the structures of **1** and **2** at B3LYP/6-31G(d) obtained by Ajami et al.[11] have been used as the initial geometries of the optimization process. The average (hyper)polarizabilities are defined by following equations:[22]

$$\overline{\alpha} = \frac{1}{3}\sum_{i=x,y,z}\alpha_{ii} \tag{1}$$

$$\overline{\beta} = \frac{1}{5|\overline{\mu}|}\sum_{i=x,y,z}\mu_i(\beta_{ijj} + \beta_{jij} + \beta_{jji}) \tag{2}$$

and

$$\overline{\gamma} = \frac{1}{15}\sum_{i,j=x,y,z}\gamma_{iijj} + \gamma_{ijij} + \gamma_{ijji} \tag{3}$$

The vibrational (hyper)polarizabilities can be computed using the pioneer perturbation treatment of Bishop and Kirtman[45] or the variational approach based on analytical response theory, proposed by Christiansen et al.[46] One approach intertwined with the BK method is the nuclear relaxation approach, whose derivation of vibrational NLOP formulas is based on determining the change equilibrium geometry induced by a static external field.[47,48] Even though there is an exact correspondence between the BK perturbation treatment and the nuclear relaxation approach, the latter has spawned valuable new concepts and related computational procedures. From the viewpoint of the nuclear relaxation (NR) procedure, it is natural to divide the total vibrational (hyper)polarizability into nuclear relaxation (P^{nr}) and curvature (P^c) contributions. P^{nr} and P^c arise from the change in the electronic and zero-point vibrational averaging corrections caused by the field-induced relaxation of the equilibrium geometry, respectively. The P^c is usually smaller and far more computationally expensive than P^{nr},[24,26] and it is not computed here.

Under the infinite optical frequency (IOF) approximation, which corresponds to the limit $\omega \rightarrow \infty$, the expression for the dynamic P^{nr} can be obtained using the nuclear relaxation approach. Tests of the IOF approximation have shown that it yields satisfactory results.[49,50] The bottleneck in calculating P^{nr} from analytical expressions is the number and the computational cost of the nth-order derivatives with respect to normal modes.[48] Their number is on the order of $(3N-6)^n$, with N being the number of atoms. This problem can be circumvented by using the finite field nuclear relaxations approach or by introducing a set of static field-induced vibrational coordinates (FICs), which are just the displacement coordinates derived from the change in the equilibrium geometry induced by a static applied field.[50−52] The FICs radically reduce the number of nth-order derivatives to be evaluated. For instance, for the nuclear relaxation contribution to Pockels effect, the analytical expressions containing sums over $3N-6$ normal coordinates can be reduced to formulas that involve only three FICs.

The analytical definitions of the first (χ_1^{α}) and harmonic second-order ($\chi_{2,har}^{\alpha\beta}$) FICs are based on the expansion of the field-dependent displacement of the field-free normal coordinate (Q_i^F) induced by a uniform static electric field as a power series in the field (F_α). The expressions of χ_1^{α} and $\chi_{2,har}^{\alpha\beta}$ are given by[52] nuclear coordinates

$$\chi_1^{\alpha} = \sum_{i=1}^{3N-6}\frac{\partial Q_i^F}{\partial F_\alpha}Q_i \tag{4}$$

and

$$\chi_{2,\mathrm{har}}^{\alpha\beta} = \sum_{i=1}^{3N-6}\left(\frac{\partial^2 Q_i^F}{\partial F_\alpha \partial F_\beta}\right)_{\mathrm{har}}Q_i \tag{5}$$

dx.doi.org/10.1021/ct2005424 |J. Chem. Theory Comput. 2011, 7, 3935–3943

Table 1. Selected Geometrical Parameters of the Bianthraquinodimethane Modified [16]Annulene with Hückel Topology Calculated Using the 6-31+G(d) Basis Set and Seven Different Levels of Theory (All Quantities in Ångstroms)

distances[a]	HF	B3LYP	BHandHLYP	BMK	M052X	CAM-B3LYP	MP2
d_1	1.341	1.366	1.350	1.365	1.355	1.354	1.372
d_2	1.502	1.496	1.490	1.502	1.492	1.494	1.481
d_3	1.402	1.417	1.404	1.418	1.408	1.408	1.416
d_4	1.491	1.485	1.480	1.492	1.482	1.484	1.475
d_5	1.334	1.359	1.343	1.358	1.349	1.347	1.368
d_6	1.471	1.456	1.455	1.466	1.459	1.460	1.448
d_7	1.329	1.351	1.336	1.350	1.343	1.341	1.358
d_8	1.490	1.485	1.480	1.494	1.485	1.483	1.482
d_9	1.326	1.345	1.332	1.346	1.338	1.337	1.352
d_{10}	1.494	1.487	1.482	1.494	1.485	1.487	1.480
d_{11}	1.405	1.420	1.407	1.422	1.412	1.411	1.420
d_{12}	1.502	1.496	1.490	1.501	1.491	1.494	1.480
BLA	0.139	0.110	0.120	0.118	0.118	0.120	0.096

[a] For the numbering of the distances, see Figure 2.

Table 2. Selected Geometrical Parameters of the Bianthraquinodimethane Modified [16]Annulene with the Möbius Topology Calculated Using the 6-31+G(d) Basis Set and Seven Different Levels of Theory (All Quantities in Ångstroms)

distances[a]	HF	B3LYP	BHandHLYP	BMK	M052X	CAM-B3LYP	MP2	exptl[b]
d_1	1.338	1.363	1.347	1.362	1.353	1.352	1.373	1.353
d_2	1.497	1.491	1.485	1.496	1.486	1.489	1.475	1.488
d_3	1.400	1.416	1.402	1.417	1.406	1.407	1.415	1.411
d_4	1.494	1.486	1.482	1.493	1.483	1.486	1.474	1.485
d_5	1.336	1.364	1.346	1.362	1.353	1.351	1.373	1.355
d_6	1.462	1.445	1.446	1.456	1.450	1.450	1.436	1.449
d_7	1.334	1.362	1.344	1.360	1.351	1.349	1.370	1.350
d_8	1.475	1.458	1.459	1.469	1.463	1.463	1.454	1.452
d_9	1.336	1.364	1.346	1.362	1.354	1.351	1.374	1.332
d_{10}	1.493	1.486	1.481	1.493	1.484	1.485	1.475	1.485
d_{11}	1.407	1.421	1.408	1.423	1.413	1.412	1.422	1.412
d_{12}	1.503	1.497	1.491	1.503	1.493	1.495	1.483	1.489
BLA	0.130	0.094	0.108	0.103	0.105	0.107	0.077	0.104
SDD	0.014	0.012	0.007	0.014	0.008	0.007	0.018	

[a] For the numbering of the distances, see Figure 2. [b] The experimental distances are obtained from the X-ray crystal structure, see ref 9.

Only one first order FIC is required to calculate each diagonal component of α^{nr} (0; 0), β^{nr} (0;0,0), β^{nr} $(\omega;\omega,0)_{\omega\to\infty}$ (IOF approximation NR Pockels β), and γ^{nr} $(-2\omega;\omega,\omega,0)_{\omega\to\infty}$ (IOF approximation NR field induced second harmonic (FISH) γ) tensors. Also, one unique FIC, but now the harmonic second order FIC, is necessary to calculate each diagonal component of γ^{nr} $(-\omega;\omega,-\omega,\omega)_{\omega\to\infty}$ (IOF approximation NR intensity-dependent refractive index (IDRI) γ). Using only two FICs, a first order and a harmonic second order FIC, one can also obtain each diagonal component of γ^{nr} $(-\omega;\omega, 0,0)_{\omega\to\infty}$ (IOF approximation NR Kerr effect γ). The calculation of γ^{nr} (0;0,0,0) requires second order FICs instead of harmonic second order FICs. The calculation of second order FICs is very expensive, and the static NR second hyperpolarizabilities have not been calculated here. The Supporting Information contains the plots and analysis of the no-mass-weighted orthonormal FICs of the Hückel and Möbius conformations evaluated at the CAM-B3LYP/6-31+G(d) level.

3. RESULTS AND DISCUSSION

Tables 1 and 2 show some selected bond lengths of the Hückel (structure **1**) and Möbius (structure **2**) topologies, respectively, using the 6-31+G(d) basis set and seven different levels of theory. The C−C bond lengths determined from X-ray crystallography are only reported for the Möbius structure.[9] Tables 1 and 2 also contain the bond length alternation (BLA, the average difference between simple and double bond lengths) along the [16]annulene circuit of **1** and **2** structures. In both topologies, there are three possible [16]annulene paths. The BLA differences between the three paths are very small, less than 0.01 Å. Finally, Table 2 also includes the standard deviation of the distances (SDD), which is defined as

$$\mathrm{SDD} = \sqrt{\sum_{i=1}^{N} \frac{(d_i - d_{i,\mathrm{exp}})^2}{N-1}} \qquad (6)$$

Table 3. Electronic Polarizabilities and First and Second Hyperpolarizabilities of the Bianthraquinodimethane Modified [16] Annulene with Hückel Topology Calculated Using the 6-31+G(d) Basis Set and Seven Different Levels of Theory (All Quantities in Atomic Units)[a]

properties	HF	B3LYP	BHandHLYP	BMK	M052X	CAM-B3LYP	MP2
$\alpha^{e}_{xx}(0;0)$	3.68×10^{2}	3.90×10^{2}	3.71×10^{2}	3.75×10^{2}	3.65×10^{2}	3.74×10^{2}	3.58×10^{2}
$\alpha^{e}_{yy}(0;0)$	4.23×10^{2}	4.74×10^{2}	4.41×10^{2}	4.57×10^{2}	4.44×10^{2}	4.47×10^{2}	4.54×10^{2}
$\alpha^{e}_{zz}(0;0)$	4.00×10^{2}	4.45×10^{2}	4.18×10^{2}	4.34×10^{2}	4.23×10^{2}	4.24×10^{2}	4.30×10^{2}
$\overline{\alpha}^{e}(0;0)$	3.97×10^{2}	4.36×10^{2}	4.10×10^{2}	4.22×10^{2}	4.10×10^{2}	4.15×10^{2}	4.14×10^{2}
$\beta^{e}_{yyy}(0;0,0)$	9.13×10^{1}	2.52×10^{2}	1.57×10^{2}	1.41×10^{2}	1.07×10^{2}	1.39×10^{2}	1.69×10^{2}
$\beta^{e}_{zzz}(0;0,0)$	4.90×10^{1}	1.80×10^{2}	1.07×10^{2}	9.22×10^{1}	6.90×10^{1}	8.97×10^{1}	1.08×10^{2}
$\overline{\beta}^{e}(0;0,0)$	-9.71×10^{1}	-2.75×10^{2}	-1.78×10^{2}	-1.88×10^{2}	-1.46×10^{2}	-1.67×10^{2}	-2.16×10^{2}
$\gamma^{e}_{xxxx}(0;0,0,0)$	7.59×10^{4}	1.82×10^{5}	1.15×10^{5}	1.38×10^{5}	1.18×10^{5}	1.20×10^{5}	1.53×10^{5}
$\gamma^{e}_{yyyy}(0;0,0,0)$	1.36×10^{5}	3.08×10^{5}	2.10×10^{5}	2.22×10^{5}	2.11×10^{5}	2.17×10^{5}	2.76×10^{5}
$\gamma^{e}_{zzzz}(0;0,0,0)$	9.00×10^{4}	2.09×10^{5}	1.38×10^{5}	1.39×10^{5}	1.38×10^{5}	1.43×10^{5}	1.74×10^{5}
$\overline{\gamma}^{e}(0;0,0,0)$	3.38×10^{4}	7.81×10^{4}	5.14×10^{4}	5.44×10^{4}	5.13×10^{4}	5.35×10^{4}	

[a] $\beta^{e}_{xxx}(0;0,0)$ is null by symmetry.

Table 4. Electronic Polarizabilities and First and Second Hyperpolarizabilities of the Bianthraquinodimethane Modified [16] Annulene with the Möbius Topology Calculated Using the 6-31+G(d) Basis Set and Seven Different Levels of Theory (All Quantities in Atomic Units)[a]

properties	HF	B3LYP	BHandHLYP	BMK	M052X	CAM-B3LYP	MP2
$\alpha^{e}_{xx}(0;0)$	3.89×10^{2}	4.52×10^{2}	4.18×10^{2}	4.43×10^{2}	4.32×10^{2}	4.26×10^{2}	4.52×10^{2}
$\alpha^{e}_{yy}(0;0)$	4.39×10^{2}	4.93×10^{2}	4.58×10^{2}	4.73×10^{2}	4.60×10^{2}	4.63×10^{2}	4.62×10^{2}
$\alpha^{e}_{zz}(0;0)$	3.71×10^{2}	3.91×10^{2}	3.69×10^{2}	3.70×10^{2}	3.54×10^{2}	3.72×10^{2}	3.49×10^{2}
$\overline{\alpha}^{e}(0;0)$	4.00×10^{2}	4.45×10^{2}	4.15×10^{2}	4.29×10^{2}	4.15×10^{2}	4.20×10^{2}	4.21×10^{2}
$\beta^{e}_{yyy}(0;0,0)$	-8.25×10^{1}	-2.75×10^{2}	-1.92×10^{2}	-2.61×10^{2}	-2.50×10^{2}	-2.22×10^{2}	-5.31×10^{2}
$\overline{\beta}^{e}(0;0,0)$	9.26×10^{1}	3.40×10^{2}	2.21×10^{2}	-3.37×10^{2}	-2.71×10^{2}	2.41×10^{2}	-5.13×10^{2}
$\gamma^{e}_{xxxx}(0;0,0,0)$	9.15×10^{4}	2.27×10^{5}	1.43×10^{5}	1.45×10^{5}	1.38×10^{5}	1.48×10^{5}	1.75×10^{5}
$\gamma^{e}_{yyyy}(0;0,0,0)$	9.57×10^{4}	2.45×10^{5}	1.62×10^{5}	1.66×10^{5}	1.68×10^{5}	1.75×10^{5}	2.67×10^{5}
$\gamma^{e}_{zzzz}(0;0,0,0)$	9.59×10^{4}	2.23×10^{5}	1.40×10^{5}	1.37×10^{5}	1.31×10^{5}	1.42×10^{5}	1.65×10^{5}
$\overline{\gamma}^{e}(0;0,0,0)$	3.88×10^{4}	1.00×10^{5}	6.27×10^{4}	6.95×10^{4}	6.77×10^{4}	6.57×10^{4}	

[a] $\beta^{e}_{xxx}(0;0,0)$ and $\beta^{e}_{zzz}(0;0,0)$ are null by symmetry.

where d_i and $d_{i,exp}$ are the calculated and experimental bond distances, respectively, and N is the number of bond lengths considered (N = 12). From the BLA and SDD values, one can easily see that a better geometrical description of the [16]annulene path is obtained with the BHandHLYP, M052X, and CAM-B3LYP methodologies than using HF, B3LYP, BMK, and MP2 treatments.

Moreover, Tables 1 and 2 show that HF is the method that predicts the shortest double bonds and the longest single bonds along the [16]annulene circuit, i.e., the largest BLA value. On the other hand, MP2 is the method that predicts the longest double bonds and the shortest single bonds, i.e., the smallest BLA value. The bond distances calculated from the B3LYP and BMK approaches are larger than the experimental ones. It is worth noting that the BHandHLYP and CAM-B3LYP methods show the smallest values of SDD, although BHandHLYP predicts a slightly large BLA. Finally, the M052X treatment obtains the closest BLA distance to the experimental value.

According to the results displayed in Table 2, one can conclude that M052X, BHandHLYP, and CAM-B3LYP levels of theory provide an accurate reproduction of the X-ray crystal structure of the bianthraquinodimethane modified [16]annulene with Möbius topology.

Tables 3 and 4 contain the electronic contribution to α, β, and γ for the structures **1** and **2**, respectively, using the 6-31+G(d) basis set and seven different levels of theory. For each property, the diagonal components and the average values, see eqs 1−3, are reported. As one can easily see, the first hyperpolarizabilities of these two conformations are quite small, and no relevant conclusions can be obtained. In addition, the terms of the dipole moment, which have not been reported in the Tables 3 and 4, are also negligible (it is important to remember that conformations **1** and **2** show C_S and C_2 symmetry, respectively, and some diagonal terms are null by symmetry). Then, in the following paragraphs our analysis will focus on α and γ values. The evaluation of $\overline{\gamma}^{e}$ has not been reported at the MP2 level due to computational limitations; i.e., $\overline{\gamma}^{e}$ requires terms like γ^{e}_{iijj}, see eq 3, which are not easy to evaluate from the finite field differentiation of μ^{e}.

In Tables 3 and 4, one can notice the electronic correlation results essential for the correct evaluation of the NLOP. For instance, the MP2 and CAM-B3LYP methodologies increase γ^{e} values around 100% and 60% with respect to the HF level (around 10% for α^{e} values). The MP2 results show larger α^{e} and γ^{e} values than HF, BHandHLYP, BMK, M052X, and CAM-B3LYP methods and smaller values than B3LYP. Although in the literature it has been reported that MP2 treatment often yields a significant fraction of the electron correlation contribution of the NLOP,[25,26] it has also been shown that the MP2 approach overestimates by more than a factor of 2 with respect to CCSD(T) for

Table 5. Nuclear Relaxation Polarizabilities and First Hyperpolarizabilities of the Bianthraquinodimethane Modified [16] Annulene with the Hückel and Möbius Topologies Calculated at HF and CAM-B3LYP Levels of Theory Using the 6-31+G(d) Basis Set (All Quantities in Atomic Units)[a]

	HF		CAM-B3LYP	
	Hückel	Möbius	Hückel	Möbius
$\alpha^{nr}_{xx}(0;0)$	2.70×10^1	1.68×10^1	3.19×10^1	1.20×10^1
$\alpha^{nr}_{yy}(0;0)$	1.34×10^1	9.92×10^0	1.31×10^1	9.30×10^0
$\alpha^{nr}_{zz}(0;0)$	1.01×10^1	1.69×10^1	1.08×10^1	2.18×10^1
$\overline{\alpha}^{nr}(0;0)$	1.69×10^1	1.46×10^1	1.86×10^1	1.44×10^1
$\beta^{nr}_{yyy}(0;0,0)$	-1.30×10^2	-2.63×10^2	-2.10×10^2	-2.55×10^2
$\beta^{nr}_{zzz}(0;0,0)$	-4.04×10^2		-5.51×10^2	
$\overline{\beta}^{nr}(0;0,0)$	3.48×10^2	5.83×10^2	1.92×10^3	7.45×10^2
$\beta^{nr}_{yyy}(-\omega;\omega,0)_{\omega\to\infty}$	-6.96×10^1	-8.16×10^1	-9.06×10^1	-8.38×10^1
$\beta^{nr}_{zzz}(-\omega;\omega,0)_{\omega\to\infty}$	-1.63×10^2		-2.13×10^2	
$\overline{\beta}^{nr}(-\omega;\omega,0)_{\omega\to\infty}$	1.24×10^2	2.07×10^2	6.11×10^2	2.62×10^2

[a] $\beta^{nr}_{xxx}(0;0,0)$ and $\beta^{nr}_{xxx}(-\omega;\omega,0)_{\omega\to\infty}$ are null by symmetry, and $\beta^{nr}_{zzz}(0;0,0)$ and $\beta^{nr}_{zzz}(-\omega;\omega,0)_{\omega\to\infty}$ are also null by summetry, but only at the Möbius conformation.

Table 6. Nuclear Relaxation Second Hyperpolarizabilities of the Bianthraquinodimethane Modified [16] Annulene with the Hückel and Möbius Topologies Calculated at HF and CAM-B3LYP Levels of Theory Using the 6-31+G(d) Basis Set (All Quantities in Atomic Units)

	HF		CAM-B3LYP	
	Hückel	Möbius	Hückel	Möbius
$\gamma^{nr}_{xxxx}(-\omega;\omega,0,0)_{\omega\to\infty}$	1.00×10^5	3.48×10^4	1.74×10^5	4.05×10^4
$\gamma^{nr}_{yyyy}(-\omega;\omega,0,0)_{\omega\to\infty}$	5.58×10^4	8.11×10^4	6.69×10^4	1.08×10^5
$\gamma^{nr}_{zzzz}(-\omega;\omega,0,0)_{\omega\to\infty}$	4.46×10^4	3.07×10^4	6.23×10^4	6.45×10^4
$\overline{\gamma}^{nr}(-\omega;\omega,0,0)_{\omega\to\infty}$[a,b]	1.16×10^5	1.06×10^5	6.07×10^5	1.44×10^5
$\gamma^{nr}_{xxxx}(-2\omega;\omega,\omega,0)_{\omega\to\infty}$	3.92×10^3	1.86×10^3	4.93×10^3	1.38×10^3
$\gamma^{nr}_{yyyy}(-2\omega;\omega,\omega,0)_{\omega\to\infty}$	2.11×10^3	6.67×10^2	1.56×10^3	3.44×10^2
$\gamma^{nr}_{zzzz}(-2\omega;\omega,\omega,0)_{\omega\to\infty}$	1.68×10^3	2.02×10^3	1.75×10^3	2.98×10^3
$\overline{\gamma}^{nr}(-2\omega;\omega,\omega,0)_{\omega\to\infty}$	2.73×10^3	2.04×10^3	2.48×10^3	2.02×10^3
$\gamma^{nr}_{xxxx}(-\omega;\omega,-\omega,\omega)_{\omega\to\infty}$	1.75×10^5	6.29×10^4	2.41×10^5	7.89×10^4
$\gamma^{nr}_{yyyy}(-\omega;\omega,-\omega,\omega)_{\omega\to\infty}$	9.94×10^4	1.61×10^5	1.22×10^5	2.19×10^5
$\gamma^{nr}_{zzzz}(-\omega;\omega,-\omega,\omega)_{\omega\to\infty}$	8.39×10^4	5.52×10^4	1.19×10^5	1.20×10^5
$\overline{\gamma}^{nr}(-\omega;\omega,-\omega,\omega)_{\omega\to\infty}$[a]	2.17×10^5	1.21×10^5	5.49×10^5	1.68×10^5

[a] The $[\alpha^2]$ terms were calculated using $3N-6$ normal modes instead of the six first (χ^{α}_1) and harmonic second-order ($\chi^{\alpha\alpha}_{2,har}$) FICs in order to obtain the correct value for the nondiagonal elements of the hyperpolarizability tensor (see Table 1 of ref 52 for more details). [b] The nondiagonal elements of the $[\mu^2\alpha]$ term are approximate. The exact calculation of such elements requires using either second-order $\chi^{xy}_{2,har}$, $\chi^{xz}_{2,har}$, and $\chi^{yz}_{2,har}$ FICs or the $3N-6$ normal coordinates (see Table 1 of ref 52 for more details).

polybutatriene chains.[53] In the previous paragraphs, we have shown that MP2 methodology predicts a Möbius geometry with the largest SDD value (0.018 Å) with respect to the X-ray crystal structure. Then, one can conclude that for these systems the MP2 level cannot be considered as a reference model for the evaluation of the NLOP.

Among the seven methods used in this work, the HF and B3LYP methods present the smallest and largest, respectively, values of α^e and γ^e. The overestimation of the second hyperpolarizabilities using the B3LYP approach is expected due to the incorrect electric field dependence modeled by the conventional exchange functional treatments.[28] On the other hand, the four remaining DFT methods used in this work (BHandHLYP, BMK, M052X, and CAM-B3LYP) show intermediate values of α^e and γ^e between HF and B3LYP levels. It is worth noting that α^e and γ^e values obtained with these four DFT treatments are very similar; i.e., the differences between them are always smaller than 20%. It is important to remember that BHandHLYP, M052X, and CAM-B3LYP levels correctly reproduce the X-ray crystal structure of bianthraquinodimethane modified [16]annulene with Möbius topology. To validate the NLOP results obtained using these four DFT methodologies, it would be necessary to evaluate them using coupled cluster methods results, although they are computationally prohibitive for **1** and **2** structures. Nevertheless, several works[32,33] have shown that DFT functionals with a large fraction of Hartree−Fock and DFT long-range functionals remove the overestimation of polarizabilities and hyperpolarizabilities by standard DFT. Moreover, it has been found that CAM-B3LYP results are very similar to the desirable coupled cluster methods.[33] We conclude that the results of this

work are encouraging to the evaluation of the NLOP for larger Hückel−Möbius switches, because it seems that BHandHLYP, M052X, and CAM-B3LYP methods can provide semiquantitative accuracy with a reasonable computational cost.

The diagonal components of α and γ for the Möbius and Hückel topologies are quite similar. Only the y direction (more or less the direction that goes through the [16]annulene circuit) shows slightly higher values than x and z directions; e.g., in the Hückel conformation, $\gamma^{e}_{yyyy}(0;0,0,0)$ is between 35 and 45% larger than $\gamma^{e}_{xxxx}(0;0,0,0)$ and $\gamma^{e}_{zzzz}(0;0,0,0)$ for the seven different levels of theory, see Table 3. Moreover, it is worth noting that the $\overline{\alpha}^{e}$ and $\overline{\gamma}^{e}$ values for the Hückel and Möbius conformations are also very similar between them. The maximum difference is obtained at the M052X level with a $\overline{\gamma}^{e}(0;0,0,0)_{\text{Hückel}}/\overline{\gamma}^{e}(0;0,0,0)_{\text{Möbius}}$ ratio of 0.76. This conclusion shows a direct link with the controversial issue about the aromaticity character of these systems. Our calculations agree well with previous results[9,11,12] that **1** and **2** structures present similar electronic and magnetic properties.

In Tables 5 and 6 are reported the static and dynamic nuclear relaxation polarizabilities and first and second hyperpolarizabilitites for structures **1** and **2**. Our analysis has been focused on only two methodologies (HF and CAM-B3LYP), because the evaluation of the vibrational contribution to NLOP implies an important computational effort (each conformation requires 13 frequency calculations). These two treatments have been selected to check the differences between the HF level and a theoretical approach that correctly describes the geometry and the electronic contribution to NLOP. The CAM-B3LYP method was chosen, although as we have seen in previous paragraphs M052X and BHandHLYP could also have been good choices. In a similar way to the electronic contribution, CAM-B3LYP treatment gives important augmentations for $\overline{\gamma}^{nr}$ with respect to the values obtained at the HF level, e.g., $\overline{\gamma}^{nr}(-\omega;\omega,0,0)_{\omega\to\infty}$ and $\overline{\gamma}^{nr}(-\omega;\omega,-\omega,\omega)_{\omega\to\infty}$ at the Hückel conformation increase around 400% and 150%, respectively.

In contrast to Tables 3 and 4, important differences are found between the diagonal components of nuclear relaxation α and γ for Hückel and Möbius topologies. For instance, at the CAM-B3LYP level in the Möbius conformation, $\alpha^{nr}_{zz}(0;0)$ is 1.8 and 2.3 times larger than $\alpha^{nr}_{xx}(0;0)$ and $\alpha^{nr}_{yy}(0;0)$, respectively (see Table 5), and $\gamma^{nr}_{yyyy}(-\omega;\omega,0,0)_{\omega\to\infty}$ is 2.7 and 1.7 times larger than in the x and z directions, respectively (see Table 6). In analogy to the electronic contribution, $\overline{\alpha}^{nr}$ and $\overline{\gamma}^{nr}$ values for the Hückel and Möbius conformations are quite similar between them using the HF treatment; i.e., the maximum difference is the ratio $\overline{\gamma}^{nr}(-2\omega;\omega,\omega,0)_{\text{Hückel}}/\overline{\gamma}^{nr}(-2\omega;\omega,\omega,0)_{\text{Möbius}}$ with a value of 1.8. However, CAM-B3LYP results show two important exceptions of this tendency, the average IOF approximation NR Kerr and IDRI effects, which present ratios of 4.2 and 3.3, respectively.

Last but not least, we analyze the relevance of the vibrational contribution to NLOP with respect to the electronic contribution. According to Tables 3−6, it is clear that $\overline{\alpha}^{nr}(0;0)$ and $\overline{\gamma}^{nr}(-2\omega;\omega,\omega,0)_{\omega\to\infty}$ corrections are not negligible, though they are less than 10% of the corresponding static electronic properties. Moreover, $\overline{\gamma}^{nr}(-\omega;\omega,0,0)_{\omega\to\infty}$ and $\overline{\gamma}^{nr}(-\omega;\omega,-\omega,\omega)_{\omega\to\infty}$ are either larger than or comparable in size to $\overline{\gamma}^{e}(0;0,0,0)$. For instance, the IOF approximation of NR IDRI averages of structures **1** and **2** evaluated at the CAM-B3LYP level are 10.2 and 2.6, respectively, larger than the electronic contribution. Then, one can conclude that an accurate evaluation of NLOP for annulenes with Hückel and Möbius topologies requires the study of the vibrational contribution. In addition, the sum of the electronic and vibrational contributions ($\overline{\gamma} = \overline{\gamma}^{e} + \overline{\gamma}^{vib}$) shows that the structures **1** and **2** present high values of NLOP, i.e., values around 5×10^5.

4. SUMMARY AND CONCLUSIONS

We have investigated the electronic and vibrational contributions to static and dynamic NLOP of the bianthraquinodimethane modified [16]annulene with C_S Hückel (structure **1**) and C_2 Möbius (structure **2**) topologies synthesized by Herges and co-workers. The calculations were performed at the HF, B3LYP, BHandHLYP, BMK, M052X, CAM-B3LYP, and MP2 levels with the 6-31+G(d) basis set. No analogous treatments of NLOP for these systems have been carried out as far as we know. The results of this work lead us to the following conclusions:

a. Among the seven treatments considered in this work, the BHandHLYP, M052X, and CAM-B3LYP levels correctly reproduce the X-ray crystal structure of the annulene with Möbius topology. On the contrary, the HF, MP2, and B3LYP methods predict structural conformations, which show important divergences with respect to the experimental results.
b. In the study of the electronic contribution to NLOP, it has been found that BHandHLYP, M052X, and CAM-B3LYP methods provide similar results. On the other hand, HF (MP2 and B3LYP) underestimates (overestimate) the NLOP. In the literature, it has been reported that CAM-B3LYP agrees with CCSD(T). Then, we conclude that BHandHLYP, M052X, and CAM-B3LYP can provide semiquantitative results with a reasonable computational cost for the evaluation of NLOP with Hückel−Möbius switches.
c. $\overline{\alpha}$ and $\overline{\gamma}$ values for Hückel and Möbius conformations are similar. Our results for the NLOP agree with literature results that both Hückel and Möbius structures have similar electronic and magnetic properties.
d. The vibrational contribution to static and dynamic NLOP for Möbius−Hückel systems can be either larger or comparable in size than the electronic contribution, and it must to be considered for an accurate evaluation of the NLOP.

The experience obtained in this work will be very useful for the photophysical characterization of new topologically switchable porphyrins with high NLOPs (see refs 15−18), which show a clear relationship between aromaticity, molecular geometry, and NLOP. The key factors, which will determine their potential as optical switches, will be the high values and the large differences of NLOP between the Möbius and Hückel conformations. These systems present a considerable number of atoms (around 150 atoms), and therefore, the choice of an adequate methodology for the electronic and vibrational contributions is essential for the correct prediction of the NLOP. Additional work on the evaluation of new topologically switchable porphyrins (A,D-di-*p*-benzi-[28]hexaphyrin(1.1.1.1.1.1)[16] and meso-aryl-substituted [28]hexaphyrins(1.1.1.1.1.1)[18]) with high NLOP is in progress in our laboratory.

■ ASSOCIATED CONTENT

Supporting Information. Plots and analysis of χ^{α}_{1} and $\chi^{\alpha\alpha}_{2,\text{har}}$ of the Hückel and Möbius conformations evaluated at the CAM-B3LYP/6-31+G(d) level studied in this work.

This material is available free of charge via the Internet at http://pubs.acs.org.

AUTHOR INFORMATION

Corresponding Author

*Phone: +34 934006111. Fax: +34 932045903. E-mail: mtsqbm@iqac.csic.es.

ACKNOWLEDGMENT

This research has been supported by the Spanish Dirección General de Investigación Científica y Técnica (DGYCIT, grant CTQ2008-06536/BQU), the Generalitat de Catalunya (Grant 2009SGR01472), and the Research Executive Agency (Grant Agreement no. PERG05-GA-2009-249310). The calculations described in this work were carried out at the Centre de Supercomputació de Catalunya (CESCA). M.T.-S. acknowledges the CSIC for the JAE-DOC contract.

REFERENCES

(1) Fararady, M. *Trans. R. Soc. London* **1825**, *105*, 440.

(2) Minkin, V. I.; Glukhovtsev, M. N.; Simkin, B. Y. *Aromaticity and Antiaromaticity*; John Wiley & Sons: New York, 1994. Schleyer, P. v. R. *Chem. Rev.* **2001**, *101*, 1115. De Proft, F.; Geerlings, P. *Chem. Rev.* **2001**, *101*, 1451. Chen, Z. F.; Wannere, C. S.; Corminboeuf, C.; Puchta, R.; Schleyer, P. V. *Chem. Rev.* **2005**, *105*, 3842. Poater, J.; Duran, M.; Solà, M.; Silvi, B. *Chem. Rev.* **2005**, *105*, 3911.

(3) Heilbronner, E. *Tetrahedron Lett.* **1964**, 1923.

(4) Zimmerman, H. E. *J. Am. Chem. Soc.* **1966**, *88*, 1564. Castro, C.; Karney, W. L.; Valencia, M. A.; Vu, C. M. H.; Pemberton, R. P. *J. Am. Chem. Soc.* **2005**, *127*, 9704. Rzepa, H. S. *Chem. Rev.* **2005**, *105*, 3697. Pemberton, R. P.; McShane, C. M.; Castro, C.; Karney, W. L. *J. Am. Chem. Soc.* **2006**, *128*, 16692. Moll, J. F.; Pemberton, R. P.; Gutierrez, M. G.; Castro, C.; Karney, W. L. *J. Am. Chem. Soc.* **2007**, *129*, 274. Allan, C. S. M.; Rzepa, H. S. *J. Chem. Theory Comput.* **2008**, *4*, 1841. Rappaport, S. M.; Rzepa, H. S. *J. Am. Chem. Soc.* **2008**, *130*, 7613. Rzepa, H. S. *Inorg. Chem.* **2008**, *47*, 8932. Mauksch, M.; Tsogoeva, S. B. *Chem.—Eur. J.* **2010**, *16*, 7843.

(5) Hoffmann, R.; Schleyer, P. v. R.; Schaefer, H. F. *Angew. Chem., Int. Ed.* **2008**, *47*, 7164.

(6) Barborak, J. C.; Su, T. M.; Schleyer, P. v. R.; Boche, G.; Schneide, G. *J. Am. Chem. Soc.* **1971**, *93*, 279. Anastass, A. G.; Yakali, E. *J. Am. Chem. Soc.* **1971**, *93*, 3803. Anastass, A. G.; Eachus, S. W.; Yakali, E.; Elliott, R. L. *J. Chem. Soc. Chem. Commun.* **1972**, 531.

(7) Mauksch, M.; Gogonea, V.; Jiao, H.; Schleyer, P. v. R. *Angew. Chem., Int. Ed.* **1998**, *37*, 2395.

(8) Bucher, G.; Grimme, S.; Huenerbein, R.; Auer, A. A.; Mucke, E.; Kohler, F.; Siegwarth, J.; Herges, R. *Angew. Chem., Int. Ed.* **2009**, *48*, 9971.

(9) Ajami, D.; Oeckler, O.; Simon, A.; Herges, R. *Nature* **2003**, *426*, 819.

(10) Herges, R. *Chem. Rev.* **2006**, *106*, 4820.

(11) Ajami, D.; Hess, K.; Kohler, F.; Nather, C.; Oeckler, O.; Simon, A.; Yamamoto, C.; Okamoto, Y.; Herges, R. *Chem.—Eur. J.* **2006**, *12*, 5434.

(12) Castro, C.; Chen, Z. F.; Wannere, C. S.; Jiao, H. J.; Karney, W. L.; Mauksch, M.; Puchta, R.; Hommes, N.; Schleyer, P. v. R. *J. Am. Chem. Soc.* **2005**, *127*, 2425.

(13) Mohebbi, A. R.; Mucke, E. K.; Schaller, G. R.; Kohler, F.; Sonnichsen, F. D.; Ernst, L.; Nather, C.; Herges, R. *Chem.—Eur. J.* **2010**, *16*, 7767.

(14) Warner, P. M. *J. Org. Chem.* **2006**, *71*, 9271. Mauksch, M.; Tsogoeva, S. B. *Eur. J. Org. Chem.* **2008**, 5755. Wannere, C. S.; Rzepa, H. S.; Rinderspacher, B. C.; Paul, A.; Allan, C. S. M.; Schaefer, H. F.; Schleyer, P. v. R. *J. Phys. Chem. A* **2009**, *113*, 11619. Mucke, E. K.; Kohler, F.; Herges, R. *Org. Lett.* **2010**, *12*, 1708.

(15) Jux, N. *Angew. Chem., Int. Ed.* **2008**, *47*, 2543. Yoon, Z. S.; Osuka, A.; Kim, D. *Nature Chem.* **2009**, *1*, 113. Shin, J. Y.; Kim, K. S.; Yoon, M. C.; Lim, J. M.; Yoon, Z. S.; Osuka, A.; Kim, D. *Chem. Rev.* **2010**, *39*, 2751. Osuka, A.; Saito, S. *Chem. Commun.* **2011**, *47*, 4330. Saito, S.; Osuka, A. *Angew. Chem., Int. Ed.* **2011**, *50*, 4342. Stepień, M.; Sprutta, N.; Latos-Grażyński, L. *Angew. Chem., Int. Ed.* **2011**, *50*, 4288.

(16) Stepień, M.; Latos-Grażyński, L.; Sprutta, N.; Chwalisz, P.; Szterenberg, L. *Angew. Chem., Int. Ed.* **2007**, *46*, 7869.

(17) Saito, S.; Shin, J. Y.; Lim, J. M.; Kim, K. S.; Kim, D.; Osuka, A. *Angew. Chem., Int. Ed.* **2008**, *47*, 9657. Tanaka, Y.; Saito, S.; Mori, S.; Aratani, N.; Shinokubo, H.; Shibata, N.; Higuchi, Y.; Yoon, Z. S.; Kim, K. S.; Noh, S. B.; Park, J. K.; Kim, D.; Osuka, A. *Angew. Chem., Int. Ed.* **2008**, *47*, 681. Park, J. K.; Yoon, Z. S.; Yoon, M. C.; Kim, K. S.; Mori, S.; Shin, J. Y.; Osuka, A.; Kim, D. *J. Am. Chem. Soc.* **2008**, *130*, 1824. Shin, J. Y.; Lim, J. M.; Yoon, Z. S.; Kim, K. S.; Yoon, M. C.; Hiroto, S.; Shinokubo, H.; Shimizu, S.; Osuka, A.; Kim, D. *J. Phys. Chem. B* **2009**, *113*, 5794. Kim, K. S.; Yoon, Z. S.; Ricks, A. B.; Shin, J. Y.; Mori, S.; Sankar, J.; Saito, S.; Jung, Y. M.; Wasielewski, M. R.; Suka, A.; Kim, D. *J. Phys. Chem. A* **2009**, *113*, 4498. Yoon, M. C.; Cho, S.; Suzuki, M.; Osuka, A.; Kim, D. *J. Am. Chem. Soc.* **2009**, *131*, 7360. Tokuji, S.; Shin, J. Y.; Kim, K. S.; Lim, J. M.; Youfu, K.; Saito, S.; Kim, D.; Osuka, A. *J. Am. Chem. Soc.* **2009**, *131*, 7240. Inoue, M.; Kim, K. S.; Suzuki, M.; Lim, J. M.; Shin, J. Y.; Kim, D.; Osuka, A. *Angew. Chem., Int. Ed.* **2009**, *48*, 6687. Lim, J. M.; Shin, J. Y.; Tanaka, Y.; Saito, S.; Osuka, A.; Kim, D. *J. Am. Chem. Soc.* **2010**, *132*, 3105. Stepień, M.; Szyszko, B.; Latos-Grażyński, L. *J. Am. Chem. Soc.* **2010**, *132*, 3140. Tanaka, T.; Sugita, T.; Tokuji, S.; Saito, S.; Osuka, A. *Angew. Chem., Int. Ed.* **2010**, *49*, 6619. Higashino, T.; Lim, J. M.; Miura, T.; Saito, S.; Shin, J. Y.; Kim, D.; Osuka, A. *Angew. Chem., Int. Ed.* **2010**, *49*, 4950. Yoon, M. C.; Shin, J. Y.; Lim, J. M.; Saito, S.; Yoneda, T.; Osuka, A.; Kim, D. *Chem.—Eur. J.* **2011**, *17*, 6707.

(18) Sankar, J.; Mori, S.; Saito, S.; Rath, H.; Suzuki, M.; Inokuma, Y.; Shinokubo, H.; Kim, K. S.; Yoon, Z. S.; Shin, J. Y.; Lim, J. M.; Matsuzaki, Y.; Matsushita, O.; Muranaka, A.; Kobayashi, N.; Kim, D.; Osuka, A. *J. Am. Chem. Soc.* **2008**, *130*, 13568.

(19) Lim, J. M.; Yoon, Z. S.; Shin, J. Y.; Kim, K. S.; Yoon, M. C.; Kim, D. *Chem. Commun.* **2009**, 261.

(20) Xu, H. L.; Li, Z. R.; Su, Z. M.; Muhammad, S.; Gu, F. L.; Harigaya, K. *J. Phys. Chem. C* **2009**, *113*, 15380.

(21) Bishop, D. M.; Kirtman, B.; Champagne, B. *J. Chem. Phys.* **1997**, *107*, 5780.

(22) Bishop, D. M.; Norman, P. In *Handbook of Advanced Electronic and Photonic Materials*; Nalwas, H. S., Ed.; Academic: San Diego, 2001; Vol. 9, p 1.

(23) Champagne, B.; Luis, J. M.; Duran, M.; Andres, J. L.; Kirtman, B. *J. Chem. Phys.* **2000**, *112*, 1011. Kirtman, B.; Champagne, B.; Luis, J. M. *J. Comput. Chem.* **2000**, *21*, 1572. Milledori, S.; Alparone, A. *Phys. Chem. Chem. Phys.* **2000**, *2*, 2495. Champagne, B.; Spassova, M.; Jadin, J. B.; Kirtman, B. *J. Chem. Phys.* **2002**, *116*, 3935. Torrent-Sucarrat, M.; Luis, J. M.; Kirtman, B. *J. Chem. Phys.* **2005**, *122*, 204108.Luis, J. M.; Torrent-Sucarrat, M.; Christiansen, O.; Kirtman, B. *J. Chem. Phys.* **2007**, 127. Zalesny, R.; Papadopoulos, M. G.; Bartkowiak, W.; Kaczmarek, A. *J. Chem. Phys.* **2008**, *129*, 134310. Chou, C. C.; Jin, B. Y. *Chem. Phys.* **2009**, *362*, 71. Chou, C. C.; Jin, B. Y. *Theor. Chem. Acc.* **2009**, *122*, 313. Luis, J. M.; Reis, H.; Papadopoulos, M.; Kirtman, B. *J. Chem. Phys.* **2009**, *131*, 034116. Zalesny, R.; Wojcik, G.; Mossakowska, I.; Bartkowiak, W.; Avrampoulos, A.; Papadopoulos, M. G. *THEOCHEM* **2009**, *907*, 46.

(24) Torrent-Sucarrat, M.; Solà, M.; Duran, M.; Luis, J. M.; Kirtman, B. *J. Chem. Phys.* **2002**, *116*, 5363.

(25) Torrent-Sucarrat, M.; Solà, M.; Duran, M.; Luis, J. M.; Kirtman, B. *J. Chem. Phys.* **2003**, *118*, 711.

(26) Torrent-Sucarrat, M.; Solà, M.; Duran, M.; Luis, J. M.; Kirtman, B. *J. Chem. Phys.* **2004**, *120*, 6346.

(27) Loboda, O.; Zalesny, R.; Avramopoulos, A.; Luis, J. M.; Kirtman, B.; Tagmatarchis, N.; Reis, H.; Papadopoulos, M. G. *J. Phys. Chem. A* **2009**, *113*, 1159.

(28) Champagne, B.; Perpete, E. A.; van Gisbergen, S. J. A.; Baerends, E. J.; Snijders, J. G.; Soubra-Ghaoui, C.; Robins, K. A.; Kirtman, B. *J. Chem. Phys.* **1998**, *109*, 10489. van Gisbergen, S. J. A.; Schipper, P. R. T.; Gritsenko, O. V.; Baerends, E. J.; Snijders, J. G.;

Champagne, B.; Kirtman, B. *Phys. Rev. Lett.* **1999**, *83*, 694. Champagne, B.; Perpete, E. A.; Jacquemin, D.; van Gisbergen, S. J. A.; Baerends, E. J.; Soubra-Ghaoui, C.; Robins, K. A.; Kirtman, B. *J. Phys. Chem. A* **2000**, *104*, 4755.

(29) Suponitsky, K. Y.; Liao, Y.; Masunov, A. E. *J. Phys. Chem. A* **2009**, *113*, 10994.

(30) Leininger, T.; Stoll, H.; Werner, H. J.; Savin, A. *Chem. Phys. Lett.* **1997**, *275*, 151. Iikura, H.; Tsuneda, T.; Yanai, T.; Hirao, K. *J. Chem. Phys.* **2001**, *115*, 3540.Toulouse, J.; Colonna, F.; Savin, A. *Phys. Rev. A* **2004**, 70. Tawada, Y.; Tsuneda, T.; Yanagisawa, S.; Yanai, T.; Hirao, K. *J. Chem. Phys.* **2004**, *120*, 8425. Chai, J. D.; Head-Gordon, M. *J. Chem. Phys.* **2008**, *128*, 084106. Chai, J. D.; Head-Gordon, M. *Phys. Chem. Chem. Phys.* **2008**, *10*, 6615.

(31) Kamiya, M.; Sekino, H.; Tsuneda, T.; Hirao, K. *J. Chem. Phys.* **2005**, 122. Peach, M. J. G.; Cohen, A. J.; Tozer, D. J. *Phys. Chem. Chem. Phys.* **2006**, *8*, 4543. Borini, S.; Limacher, P. A.; Luthi, H. P. *J. Chem. Phys.* **2009**, *131*, 123105. Bonness, S.; Fukui, H.; Yoneda, K.; Kishi, R.; Champagne, B.; Botek, E.; Nakano, M. *Chem. Phys. Lett.* **2010**, *493*, 195. Kishi, R.; Bonness, S.; Yoneda, K.; Takahashi, H.; Nakano, M.; Botek, E.; Champagne, B.; Kubo, T.; Kamada, K.; Ohta, K.; Tsuneda, T. *J. Chem. Phys.* **2010**, *132*, 094107. de Wergifosse, M.; Champagne, B. *J. Chem. Phys.* **2011**, *134*, 074113.

(32) Jacquemin, D.; Perpete, E. A.; Medved, M.; Scalmani, G.; Frisch, M. J.; Kobayashi, R.; Adamo, C. *J. Chem. Phys.* **2007**, *126*, 191108. Jacquemin, D.; Perpete, E. A.; Scalmani, G.; Frisch, M. J.; Kobayashi, R.; Adamo, C. *J. Chem. Phys.* **2007**, *126*, 144105. Lu, S. I. *J. Comput. Chem.* **2010**, *32*, 730.

(33) Limacher, P. A.; Mikkelsen, K. V.; Luthi, H. P. *J. Chem. Phys.* **2009**, *130*, 194114.

(34) Rivera-Fuentes, P.; Aonso-Gomez, J. L.; Petrovic, A. G.; Seiler, P.; Santoro, F.; Harada, N.; Berova, N.; Rzepa, H. S.; Diederich, F. *Chem.—Eur. J.* **2011**, *16*, 9796.Cherblanc, F.; Lo, Y.; De Gussem, E.; Alcazar-Fuoli, L.; Bignell, E.; He, Y.; Chapman-Rothe, N.; Bultinck, P.; Herrebout, W. A.; Brown, R.; Rzepa, H. S.; Fuchter, M. J. *Chem. Eur. J.* DOI: 10.1002/chem.201101129.

(35) Becke, A. D. *J. Chem. Phys.* **1993**, *98*, 5648.

(36) Becke, A. D. *J. Chem. Phys.* **1993**, *98*, 1372.

(37) Boese, A. D.; Martin, J. M. L. *J. Chem. Phys.* **2004**, *121*, 3405.

(38) Zhao, Y.; Schultz, N. E.; Truhlar, D. G. *J. Chem. Theory Comput.* **2006**, *2*, 364.

(39) Yanai, T.; Tew, D. P.; Handy, N. C. *Chem. Phys. Lett.* **2004**, *393*, 51.

(40) Møller, C.; Plesset, M. S. *Phys. Rev.* **1934**, *46*, 618.

(41) Hehre, W. J.; Ditchfield, R.; Pople, J. A. *J. Chem. Phys.* **1972**, *56*, 2257.Hehre, W. J.; Radom, L.; Schleyer, P. v. R.; Pople, J. A. *Ab Initio Molecular Orbital Theory*; Wiley: New York, 1986.

(42) Frisch, M. J.; Trucks, G. W.; Schlegel, H. B.; Scuseria, G. E.; Robb, M. A.; Cheeseman, J. R.; Scalmani, G.; Barone, V.; Mennucci, B.; Petersson, G. A.; Nakatsuji, H.; Caricato, M.; Li, X.; Hratchian, H. P.; Izmaylov, A. F.; Bloino, J.; Zheng, G.; Sonnenberg, J. L.; Hada, M.; Ehara, M.; Toyota, K.; Fukuda, R.; Hasegawa, J.; Ishida, M.; Nakajima, T.; Honda, Y.; Kitao, O.; Nakai, H.; Vreven, T.; Montgomery, J. A., Jr.; Peralta, J. E.; Ogliaro, F.; Bearpark, M.; Heyd, J. J.; Brothers, E.; Kudin, K. N.; Staroverov, V. N.; Kobayashi, R.; Normand, J.; Raghavachari, K.; Rendell, A.; Burant, J. C.; Iyengar, S. S.; Tomasi, J.; Cossi, M.; Rega, N.; Millam, N. J.; Klene, M.; Knox, J. E.; Cross, J. B.; Bakken, V.; Adamo, C.; Jaramillo, J.; Gomperts, R.; Stratmann, R. E.; Yazyev, O.; Austin, A. J.; Cammi, R.; Pomelli, C.; Ochterski, J. W.; Martin, R. L.; Morokuma, K.; Zakrzewski, V. G.; Voth, G. A.; Salvador, P.; Dannenberg, J. J.; Dapprich, S.; Daniels, A. D.; Farkas, Ö.; Foresman, J. B.; Ortiz, J. V.; Cioslowski, J.; Fox, D. J. *Gaussian 09*, Revision A.1; Gaussian, Inc.: Wallingford, CT, 2009.

(43) The Hückel and Möbius conformations of bianthraquinodimethane modified [16] annulene show very small dipole moments, and we expect that the solvent will not play a crucial role in the values of NLOP.

(44) Davis, P. J.; Rabinowitz, P. In *Numerical Integration*; Blasdell: London, 1967; p 166. Champagane, B.; Kirtman, N. In *Handbook of Advanced Electronic and Photonic Materials*; Nalwas, H. S., Ed.; Academic: San Diego, 2001; Vol. 9, p 63.

(45) Bishop, D. M.; Kirtman, B. *J. Chem. Phys.* **1991**, *95*, 2646. Bishop, D. M.; Kirtman, B. *J. Chem. Phys.* **1992**, *97*, 5255. Bishop, D. M.; Luis, J. M.; Kirtman, B. *J. Chem. Phys.* **1998**, *108*, 10013.

(46) Christiansen, O. *J. Chem. Phys.* **2005**, *122*, 194105. Christiansen, O.; Kongsted, J.; Paterson, M. J.; Luis, J. M. *J. Chem. Phys.* **2006**, *125*, 214309.

(47) Bishop, D. M.; Hasan, M.; Kirtman, B. *J. Chem. Phys.* **1995**, *103*, 4157. Kirtman, B.; Luis, J. M.; Bishop, D. M. *J. Chem. Phys.* **1998**, *108*, 10008.

(48) Luis, J. M.; Marti, J.; Duran, M.; Andres, J. L.; Kirtman, B. *J. Chem. Phys.* **1998**, *108*, 4123.

(49) Bishop, D. M.; Dalskov, E. K. *J. Chem. Phys.* **1996**, *104*, 1004. Quinet, O.; Champagne, B. *J. Chem. Phys.* **1998**, *109*, 10594.

(50) Luis, J. M.; Duran, M.; Kirtman, B. *J. Chem. Phys.* **2001**, *115*, 4473.

(51) Luis, J. M.; Duran, M.; Andres, J. L.; Champagne, B.; Kirtman, B. *J. Chem. Phys.* **1999**, *111*, 875. Luis, J. M.; Champagne, B.; Kirtman, B. *Int. J. Quantum Chem.* **2000**, *80*, 471.

(52) Luis, J. M.; Duran, M.; Champagne, B.; Kirtman, B. *J. Chem. Phys.* **2000**, *113*, 5203.

(53) Kirtman, B.; Bonness, S.; Ramirez-Solis, A.; Champagne, B.; Matsumoto, H.; Sekino, H. *J. Chem. Phys.* **2008**, *128*, 114108.